Effects of Confinement on Small Water Clusters Structure and Proton Transport

P. Hirunsit and P. B. Balbuena*

Department of Chemical Engineering, Texas A&M University, College Station, Texas 77843

Received: June 20, 2007; In Final Form: August 10, 2007

Analyses of the structure of two to four water molecule clusters confined between two benzene and between two naphthalene molecules have been performed using ab initio methods. The water clusters tend to maximize the number of hydrogen bonds via formation of a cyclic network. The oxygen atoms locate approximately in the middle of the confined geometry, and the dipole vectors arrange either parallel or pointing to the surfaces. Energy barriers for proton transfer calculated for $H_3O^+-(H_2O)$ complexes in the same confined geometries suggest that there is a specific range of confinement that helps to lower the energy barriers of the proton transfer. When the walls are too close to each other, at a separation of 4 Å, the energy barriers are extremely high. Confinement does not lower the barrier energies of proton transfer when the $H_3O^+-(H_2O)$ complexes are located further from each of the surfaces by more than ∼8 Å.

1. Introduction

Water confined between hydrophobic structures reveals many interesting structural and thermodynamic properties. A proof of this is the many computational[1−8] and experimental[9,10] studies. Among those studies concerning water in model slit pores and carbon nanotubes, the X-ray diffraction experiments carried out by Iiyama and co-workers.[9,10] suggest that water molecules have an ordered, icelike structure, which is plausible along the horizontal direction of the slit pore. Similarly, Striolo et al.[11] performed simulations of water in single-walled carbon nanotubes and observed layered icelike structure. In addition, the molecular dynamics (MD) simulations performed by Koga et al.[2] showed the existence of a new ice phase, unlike any of the known bulk ice structures, which displayed a first-order transition to hexagonal and heptagonal ice nanotubes and a continuous phase transformation into solidlike square or pentagonal ice nanotubes.

The results of the MD simulations in these systems are in general significantly dependent on the water−carbon interactions. The interaction site of the carbon molecules are centered on the carbon atoms, whereas the water molecule is treated in either a single-site or a three-site representation, depending on whether the hydrogen atoms are assumed to take part in the interaction.[1] The parametrization of the available water−carbon potentials has been recently reviewed by Werder et al.[12] Pertsin and Grunze[1] concluded that a change from a single-site to a three-site potential type may strongly affect the water density in the first hydration layer and showed the preference of the linear O−H···C conformer. Also, Marti et al.[7] have performed MD simulations of liquid water embedded into two parallel graphite plates at different temperature and densities, modeled with a Lennard-Jones potential including H···C interactions. The results show two preferential orientations of the water layers close to the surfaces: the first one has one OH bond nearly parallel to the surface, and the second one has one OH bond that points to the surface. Our previous work[8] showed similar results, although the H···C interactions were not included in the force field.

Thus, a reliable model potential for the water−graphite system still needs to be developed as there are few high-quality ab initio data and surprisingly little experimental data.[13] The ab initio study by Feller and Jordan[13] applied second-order Moller−Plesset perturbation theory (MP2) to calculate the interaction energy between a water molecule and a sequence of increasing size carbon clusters from an isolated benzene molecule to a system with 37 fused benzene rings. The estimated water−graphite binding energy is slightly larger than that for the interaction between two water molecules, suggesting that the water−graphite interactions will play an important role in determining the structure of water on graphite.[13] Calculations of a water molecule sitting above a benzene ring using the MP2 with very large basis set method predicted a geometry in which the water sits above the benzene ring with the oxygen pointed away from the benzene center of mass and one of the water hydrogen atoms oriented toward the ring.[13−15] The MP2 method also showed a calculated zero-point energy of -2.9 ± 0.2 kcal/mol which is in good agreement with the experiment that yields -2.4 ± 0.1 kcal/mol.[15] Additionally, a higher level theory method, coupled cluster theory with a perturbative estimate of connected triples, CCSD(T), yielded an estimated binding energy for the water−benzene system within 0.1 kcal/mol of the value predicted by the MP2 method.[16−18]

To get more insights into the structure of confined water, this work focuses on the analyses of the geometry of water clusters located on one benzene and one naphthalene molecule, respectively, and the same water clusters placed in between two benzene and two naphthalene molecules using ab initio MP2 calculations. Furthermore, since it is well-established that water structures formed within the confinement of hydrophobic structures are a plausible effective proton-conductor medium,[19,20] a problem that is fundamental to many biological and technological processes,[21] this work also investigates the barriers for proton transfer between two water molecules confined between the model surfaces using the same calculation method. It should be noted that this is an absolutely simplified model that can help in the knowledge of water confined in graphite but that is only the first step to the full system.

* Corresponding author. E-mail: balbuena@tamu.edu.

10.1021/jp074818j CCC: $37.00
Published on Web 10/03/2007

2. Simulation Procedures

2.1. Water Clusters Confined within Model Graphite Sheets. The structure of a sequence of water clusters of increasing size $(H_2O)_n$ $n = 1-4$ confined between two parallel molecules (either benzene or naphthalene) has been investigated using ab initio calculations. Dangling bonds were terminated with hydrogen atoms to eliminate the border artifacts.[22] One important property of graphite is its aromaticity, and a finite model can describe the aromatic character of graphite well.[22] However, some properties of the presence of surface bulk structure and bulk water may be lost when a small surface model and very few water molecules are applied. Although the ab initio method provides very accurate and insightful results, it requires high computational cost that increases with the size of a system. Therefore, a balance between these factors is required. This study using the current simplified model can be the first step for a better understanding of water structures confined within graphite surfaces. Since many studies[13,14,23] have confirmed that the geometry of the complex is less sensitive to the theoretical level applied, and reasonable results are obtained already at the ab initio MP2 level, this method has been applied. The MP2 calculations were carried out along with the basis set 6-31G(d) to evaluate geometry structures of the water clusters and proton transport in the system. All the ab initio calculations were done with the GAUSSIAN 03[24] program.

Initially, the optimized geometry of water clusters $(H_2O)_n$ $n = 1-4$ on a model graphite sheet were compared with those reported by others[13,14,25] who applied a higher level of theory and with the available experimental data.[26] These water clusters $(H_2O)_n$ $n = 1-4$ in the confined system were optimized under the restriction that the in-plane $x-y$ coordinates of the benzene rings were frozen, but the z-coordinate that reflects the separation between benzene planes and water clusters was allowed to change. The studied system was built initially with two benzene rings, and subsequently with four benzene rings, to model graphite surfaces encapsulating water molecules.

2.2. Proton Transfer within the Confined System. The hydronium ion (H_3O^+) is optimized using density functional theory (DFT) calculations with the B3PW91 functional and the 6-311++g(d,p) basis set. Its optimized structure shows a flattened trigonal pyramid structure (O−H bond length 0.98 Å, H−O−H angle 113.33°). The H_3O^+ was located in the vicinity of water clusters $(H_2O)_n$ $n = 1-4$ confined between the model graphite sheets. Then, the complete system was optimized to determine where the hydrated proton locates in the confined geometry according to the MP2/6-31G(d) method/basis set.

According to the Grotthuss mechanism of proton transport[27] shown in Figure 1a, the proton propagates along the O−H···O hydrogen bond direction of the $H_3O^+-(H_2O)_n$ complexes. Li et al.[28] have studied the potential energy surface barrier (Figure 3 in ref 28) for proton transfer between two water molecules as a function of the OH distance (R_2) and parametric in the O−O distance (R_1) as defined in Figure 1b. Li et al.[28] observed that with decreasing R_1 distance between the two oxygen atoms, the activation barrier for proton transfer decreases sharply, and at a certain small R_1 value, the transfer is barrier-free. Following this model, we analyze how the energy barrier for proton transfer from a hydronium ion changes in a confined environment, as the proton propagates along the O−H···O hydrogen bond direction of the $H_3O^+-(H_2O)_n$ complexes according to the Grotthuss mechanism. At a fixed R_1 distance, the R_2 distances were scanned using the optimized geometry obtained from $H_3O^+-(H_2O)$ confined between the two graphite sheets. Then, the analysis was repeated for different values of the R_1 distance.

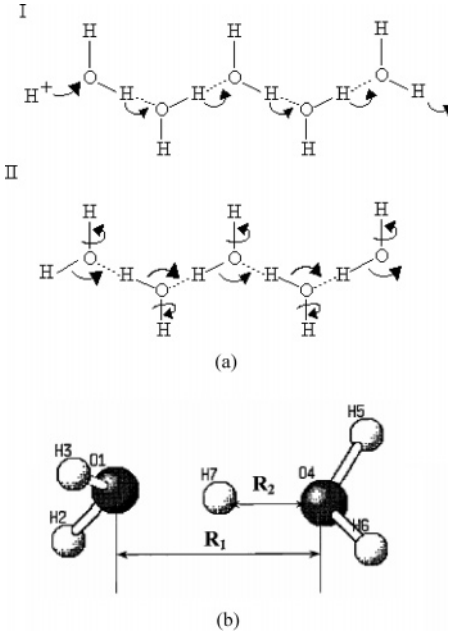

Figure 1. (a) Grotthuss mechanism of proton transport illustrating hopping (I) and turning (II) stages (ref 29). (b) Coordinates used for a potential energy surface scan (ref 28).

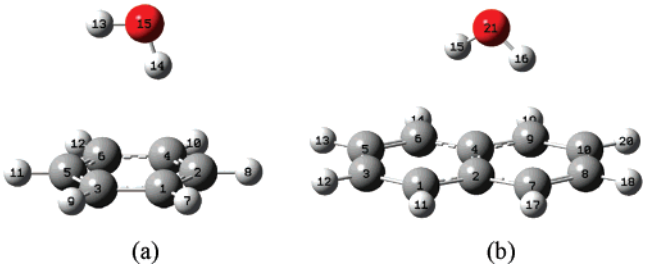

Figure 2. Optimized structures of a water molecule interacting with (a) one benzene ring and (b) two benzene rings. Note that in (a) one OH bond points to the surface and the other is parallel to it, whereas in (b) both OH bonds point to the surface. In (a), the $O_{15}H_{14}C_2$ angle is 175.87° and the distance between H_{14} and C_2 is 2.57 Å. In (b), the $O_{21}H_{15}C_5$ angle is 174.67°, $O_{21}H_{16}C_8$ is 174.85°, the distance between H_{15} and C_5 is 3.11 Å, and that between H_{16} and C_8 is 3.03 Å.

The results of the calculated potential energy surfaces for the confined systems provided an estimate of the barrier for proton transfer for confined water. Moreover, the separation distances between surfaces were varied to study if there is any influence of the proximity of the walls on the barrier.

3. Results and Discussion

3.1. Water Clusters on Model Molecular Surfaces. Optimized geometries of the benzene$-(H_2O)_n$ ($n = 1-4$) clusters are obtained from the MP2 calculations using the 6-31g(d) basis set.

3.1.1. (Benzene)−(H$_2$O). The optimized geometries of one water molecule interacting with one benzene ring, and with two benzene rings, are shown in Figure 2.

In Figure 2a, one of the O−H bonds of the water molecule points to a carbon atom of the benzene ring (the $O_{15}H_{14}C_2$ angle is 175.87°) and the other O−H bond is nearly parallel to the benzene ring. Qualitatively, these results agree with both theoretical[13,14,30] and experimental works by others.[25,26] The distance between the oxygen atom and the benzene center of mass is 3.3 Å, whereas higher level theoretical calculations at both CCSD(T)/aug-cc-pVDZ and MP2/aug-cc-pVDZ levels of

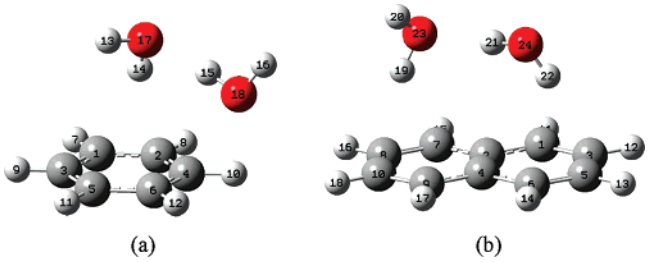

Figure 3. Optimized structures of two water molecules interacting with (a) one benzene ring and (b) two benzene rings. In (a), one OH bond ($O_{17}H_{14}$) points to the surface and the two water molecules form a H-bond. The $O_{17}H_{14}C_1$ angle is 162.42°, and the distance between H_{14} and C_1 is 2.63 Å. In (b), each water molecule has an OH bond pointing to the surface and the two water molecules form a H-bond ($O_{23}H_{21}O_{24}$) that is parallel to the surface. The angle of $O_{24}H_{22}C_5$ is 166.11°, $O_{23}H_{19}C_{10}$ is 164.62°, the distance between H_{19} and C_{10} is 2.50 Å, and that between H_{22} and C_5 is 2.68 Å.

theory give distances of 3.23 and 3.211 Å.[13] Also, the results are in good agreement with the experimentally determined value of 3.32 Å.[25,26] The distance from the center of the benzene ring to the hydrogen atom bonded to the ring is 2.5 Å, whereas higher level theoretical calculations at both CCSD(T)/aug-cc-pVDZ and MP2/aug-cc-pVDZ levels of theory yield distances of 2.417 and 2.414 Å.[13]

In the case of two benzene rings shown in Figure 2b, both O−H bonds point to neighboring carbon atoms (the $O_{21}H_{15}C_5$ angle is 174.67° and $O_{21}H_{16}C_8$ is 174.85°) in qualitative agreement with MP2/aug-cc-pVDZ results.[30] The oxygen atom is above the surface at a distance of 3.0 Å, measured as the shortest vertical distance from the oxygen atom to the surface, slightly different from the value of 3.06 Å determined from MP2/aug-cc-pVDZ[30] using seven benzene rings interacting with one water molecule. It is found that the optimized geometries obtained by the MP2 calculations using the 6-31+g(d) basis set are in good agreement with those predicted by larger basis sets.

3.1.2. (Benzene)−$(H_2O)_2$. The optimized structures of a water dimer on one and two benzene rings are shown in Figure 3.

As shown in Figure 3a, one O−H points to the surface (the $O_{17}H_{14}C_1$ angle is 162.42°) similarly to the case of one water molecule. Yet, the second water molecule is rather free from the benzene molecular surface and both of its O−H bonds point upward, forming one hydrogen bond with the other water molecule. The hydrogen bond length is 1.92 Å, slightly shorter than the results from MP2/6-31+G(d,2p), 1.93 Å.[14] The O···O separation is 2.89 Å which is close to the value of 2.94 Å calculated from QCISD/6-31+G(d,2p).[14] The hydrogen bond length of the complex is 0.034 Å shorter than that of an isolated water dimer.[14] Therefore, the water−water interaction is slightly stronger on the benzene surface. The O−H bond length associated with the hydrogen atom bonded with the surface is 0.976 Å, i.e., only 0.002 Å longer than for one water molecule. In addition, the distance of 2.43 Å between the center of the ring and the hydrogen atom bonded to the ring is 0.007 Å shorter than that in the case of one water molecule. These results suggest a slightly stronger attachment to the molecular surface in the case of two water molecules than for one water molecule, in agreement with a report[14] using MP2/6-31+G(d,2p).

Figure 3b shows the optimized structure when increasing the surface to two benzene rings. Two O−H bonds from both water molecules, $O_{23}-H_{19}$ and $O_{24}-H_{22}$, point down to the surface (the $O_{24}H_{22}C_5$ angle is 166.11°, $O_{23}H_{19}C_{10}$ is 164.62°). One O−H, $O_{23}-H_{20}$, points away from the surface, and $O_{23}\cdots H_{21}$ forms a hydrogen bond with the other water molecule. Thus,

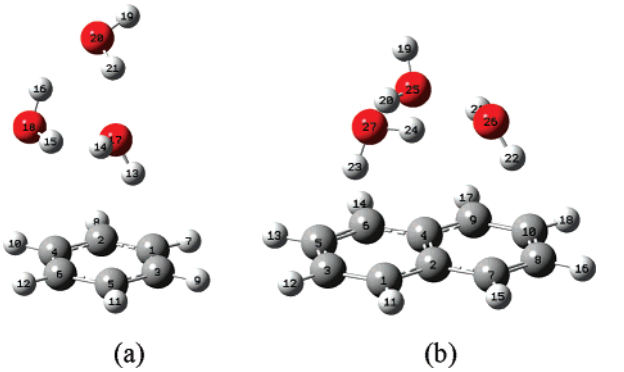

Figure 4. Optimized structures of (a) one surface of one benzene ring interacting with three water molecules and (b) one surface of two benzene rings interacting with three water molecules. In (a) there is one OH bond interacting with the surface, whereas the three H_2O molecules form a cyclic network of H-bonds. The $O_{17}H_{13}C_3$ angle is 161.97°, and the distance between H_{13} and C_3 is 2.55 Å. In (b) there are two OH bonds interacting with the surface, and the cyclic H-bond network is nearly parallel to the surface. The $O_{26}H_{22}C_8$ angle is 177.99°, $O_{27}H_{23}C_3$ is 170.88°, the distance between H_{22} and C_8 is 2.55 Å, and that between H_{23} and C_3 is 2.56 Å.

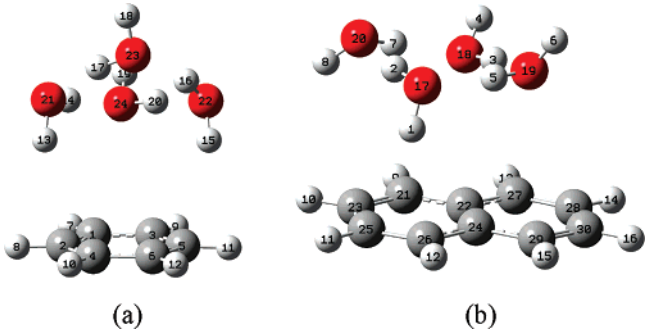

Figure 5. Optimized structures of four water molecules interacting with (a) one benzene ring and (b) two benzene rings. In case a, there are two OH bonds interacting with the benzene surface, while the water molecules form a cyclic network of H-bonds. The $O_{22}H_{15}C_5$ angle is 164.25°, $O_{21}H_{13}C_2$ is 162.72°, the distance between H_{15} and C_5 is 2.58 Å, and that between H_{13} and C_2 is 2.54 Å. In case b, it shows only one OH bond interacting with the surface. The $O_{17}H_1C_{25}$ angle is 167.11°, and the distance between H_1 and C_{25} is 2.53 Å.

both water molecules interact with the surface and with each other. The hydrogen bond length is 1.93 Å which is 0.02 Å shorter than that of the isolated water dimer and 0.015 Å longer than the case of the surface of one benzene ring. The O···O separation distance is 2.90 Å, only 0.005 longer than for the interaction with one benzene ring. The distance between O_{23} and the surface is 3.15 Å, and that between O_{24} and the surface is 3.26 Å, showing that the linear dimer is nearly parallel to the model surface. However, this feature is not found in the case of the surface modeled by one benzene ring (Figure 3a). Although the structure of $(benzene)_7-(H_2O)_2$ obtained by DFTB-D[30] shows a similar result to ours (where the linear dimer is nearly parallel to the surface), such structure differs in that there is only one O−H pointing to the surface. Our results are in good agreement with those found in QM/MD simulations using ONIOM(B3LYP/6-31+G(d):DFTB-D).[31]

3.1.3. (Benzene)−$(H_2O)_3$. Figure 4a shows the optimized geometry of three water molecules interacting with one benzene ring. The interaction of the trimer with the model surface is similar to that of the dimer and one benzene ring. There is only one O−H pointing to the surface which is $O_{17}-H_{13}$ where the angle $O_{17}H_{13}C_3$ is 161.97°. The other two water molecules are free from the surface, but all of three water molecules form a

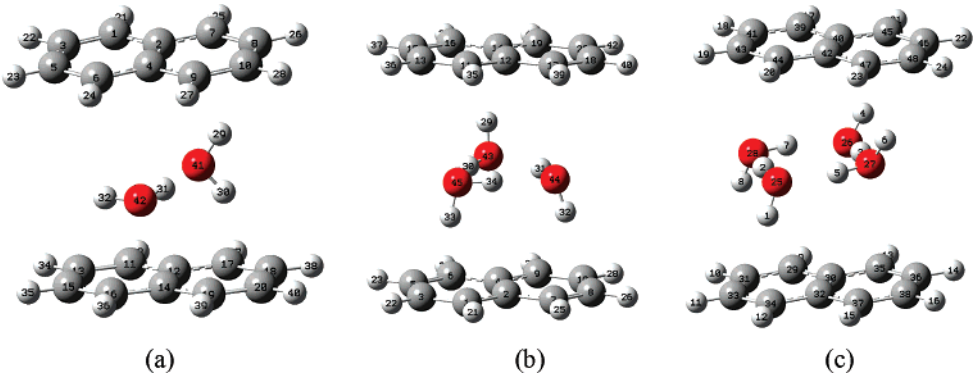

Figure 6. Optimized structures of water molecules confined within two model surfaces: (a) $(H_2O)_2$, (b) $(H_2O)_3$, and (c) $(H_2O)_4$. During the optimization process, water molecules and the *z* coordinates of benzene are allowed to move freely but the *x* and *y* coordinates of benzene are fixed. In (a) one water molecule interacts with the two surfaces; the second water molecule forms a H-bond with the first and is parallel to both surfaces. In (b) the interactions with the surface are maximized via three OH bonds pointing to them; the three waters also form a cyclic H-bond network. In (c) there are two OH bonds pointing to each of the surfaces, and the four water molecules form a square-type cycle of H-bonds.

TABLE 1: Distances in Angstroms of Water Clusters on Model Molecular Surfaces and Water Clusters Confined within Those Surfaces

	$(H_2O)_2$		$(H_2O)_3$		$(H_2O)_4$	
distance, Å	one surface[a]	two surfaces	one surface[a]	two surfaces	one surface[a]	two surfaces
O···O	2.897	2.866	O_{25}···O_{26}, 2.862 O_{26}···O_{27}, 2.811 O_{25}···O_{27}, 2.797	O_{43}···O_{44}, 2.827 O_{44}···O_{45}, 2.813 O_{45}···O_{43}, 2.797	O_{17}···O_{19}, 2.744 O_{19}···O_{18}, 2.772 O_{18}···O_{20}, 2.792 O_{20}···O_{17}, 2.807	O_{25}···O_{27}, 2.697 O_{27}···O_{26}, 2.668 O_{26}···O_{28}, 2.702 O_{28}···O_{25}, 2.731
O···H (hydrogen bonds)	1.931	1.891	O_{27}···H_{20}, 1.872 O_{25}···H_{21}, 1.977 O_{26}···H_{24}, 1.920	O_{45}···H_{30}, 1.872 O_{43}···H_{31}, 1.913 O_{44}···H_{34}, 1.898	O_{17}···H_5, 1.762 O_{19}···H_3, 1.797 O_{18}···H_7, 1.816 O_{20}···H_2, 1.841	O_{25}···H_5, 1.717 O_{27}···H_3, 1.679 O_{26}···H_7, 1.722 O_{28}···H_2, 1.764
O···surface	O_{23}, 3.147 O_{24}, 3.259 av, 3.203	O_{42}, 3.0491 O_{41}, 3.228 av, 3.139	O_{25}, 3.080 O_{26}, 3.169 O_{27}, 3.169 av, 3.139	O_{43}, 3.167 O_{44}, 3.056 O_{45}, 3.111 av, 3.111	O_{17}, 3.431 O_{18}, 2.985 O_{19}, 3.498 O_{20}, 3.610 av, 3.513	O_{25}, 3.489 O_{26}, 3.355 O_{27}, 3.534 O_{28}, 3.400 av, 3.445
H···surface	H_{19}, 2.500 H_{22}, 2.656 av, 2.578	H_{29}, 2.279 H_{30}, 2.255 av, 2.266	H_{22}, 2.545 H_{23}, 2.589 av, 2.567	H_{29}, 2.389 H_{32}, 2.389 H_{33}, 2.472 av, 2.417	H_1, 2.697 H_8, 3.000 av, 2.843	H_1, 2.563 H_8, 2.563 H_4, 2.921 H_6, 2.721 av, 2.742

[a] Water clusters on a graphite surface represented by two benzene rings.

cyclic network of hydrogen bonds. The hydrogen bonds are O_{17}···H_{15}, O_{17}···H_{21}, and O_2···H_{16} with distances of 2.21, 1.95, and 2.13 Å, respectively. The distance between O_{17} and the surface is 2.70 Å, and that between O_{18} and the surface is 2.17 Å, indicating that the O···O line is not parallel to the graphite surface. This may be because the water molecule $H_{16}O_{18}H_{15}$ is not able to interact with the benzene ring. For this reason, the simulations of confined water clusters discussed later have been done using two benzene rings modeling graphite surfaces. The distance between the center of the benzene ring and the hydrogen atom associated to the surface is 2.44 Å, which is 0.01 Å longer than for the case of two water molecules but 0.06 Å shorter than for the case of one water molecule. This suggests that the interaction between the water cluster and one benzene ring is strongest for two water molecules, of intermediate strength for three water molecules, and less strong for one water molecule. This trend agrees with the MP2/6-31+G(d,2p) calculations by Fredericks et al.[14]

Figure 4b shows the optimized structure of two benzene rings interacting with three water molecules. The interaction of the trimer with the model graphite surface is slightly different from the case of one benzene ring but similar to the case of two benzene rings interacting with two water molecules. Two O−H bonds from two water molecules, O_{26}−H_{22} and O_{27}−H_{23}, point down to the surface (the $O_{26}H_{22}C_8$ angle is 177.99°, $O_{27}H_{23}C_3$ is 170.88°), and one O−H, O_{25}−H_{19}, points away from the surface. A cyclic network of hydrogen bonds forms with O_{26}···H_{24}, O_{27}···H_{20}, and O_{25}···H_{21}. The same configuration also has been found in (benzene)$_7$−$(H_2O)_3$ using DFTB-D.[30] The distance between O_{25} and the surface is 2.81 Å, that between O_{26} and the surface is 3.08 Å, and that between O_{27} and the surface is 3.17 Å. Unlike the case of one benzene ring, these results indicate that the linear trimer is nearly parallel to this model surface and similar to the case of the water dimer. These results are in agreement with our MD simulation results shown in Figure 3 of ref 8.

TABLE 2: Average Distances between the Two Surfaces, Unit Angstroms

	$(H_2O)_2$	$(H_2O)_3$	$(H_2O)_4$
method A	6.0	6.7	6.9
method B	6.4	6.9	7.0

3.1.4. (Benzene)−$(H_2O)_4$. Figure 5a shows two O−H bonds pointing toward the surface (the $O_{22}H_{15}C_5$ angle is 164.25°, $O_{21}H_{13}C_2$ is 162.72°) and the other two O−H bonds pointing away from the surface. All four water molecules form a cyclic network of hydrogen bonds. The hydrogen bond distances, O_{21}···H_{17}, O_{23}···H_{16}, O_{22}···H_{20}, and O_{24}···H_{14}, are 1.79, 1.82, 1.79,

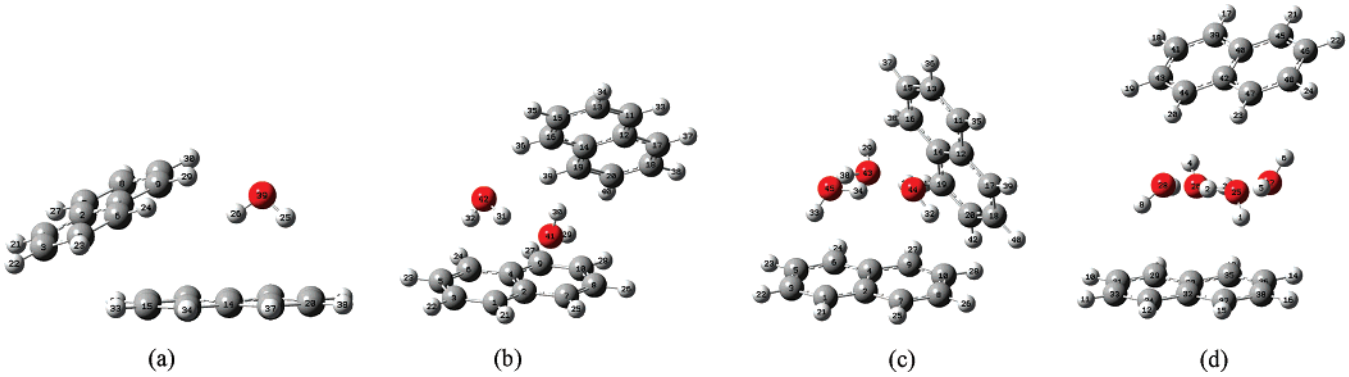

Figure 7. Optimal structures without constraints (a) H_2O, (b) $(H_2O)_2$, (c) $(H_2O)_3$, and (d) $(H_2O)_4$.

and 1.84 Å, respectively. The distance between O_{23} and the surface is 4.38 Å, and that between O_{24} and the surface is 2.55 Å. This indicates that the top water molecule does not lie parallel to the graphite surface, which is similar to the cases of dimer and trimer. The distance between the center of the benzene ring and the hydrogen atom associated to the surface is 3.08 Å, which is 0.58 Å longer than the case of one water molecule in which the water cluster has the weakest interaction (smallest contact) with the benzene molecule. Furthermore, all the O···O distances are approximately of 2.8 Å. The tetramer has a square shape linked by four hydrogen bonds, but the four water molecules are not on the same plane as found in the case of the surface modeled by two benzene rings.

Figure 5b shows that the interaction of the water tetramer with the naphthalene surface is similar to the cases of dimer and trimer. The configuration exhibits one O−H, $O_{17}-H_1$ pointing down to the surface ($O_{17}H_1C_{25}$ is 167.11°) and three O−H, $O_{20}-H_8$, $O_{18}-H_4$, and $O_{19}-H_6$, pointing away from the surface. Also, it shows a cyclic network of hydrogen bonds of $O_{17}\cdots H_5$, $O_{19}\cdots H_3$, $O_{18}\cdots H_7$, and $O_{20}\cdots H_2$. The linear tetramer is nearly parallel to the model surface as shown by the distances of 2.43, 2.98, 3.50, and 3.31 Å between O_{17}, O_{18}, O_{19}, and O_{20} and surface atoms, respectively. The water molecule, O_{17}, is nearest to the surface and shows an O−H bond pointing to the surface. The water molecule, O_{20}, is almost disconnected from the surface, resulting in the $O_{20}-H_8$ bond pointing away from the surface rather than pointing toward as was found for $(benzene)_{7-}(H_2O)_4$ using DFTB-D calculation in ref 30. Thus, a larger surface model size would be needed for studying larger water clusters. Moreover, the configuration of the tetramer is a square and all the O···O distances are approximately 2.8 Å.

3.2. Water Clusters Confined within Model Molecular Surfaces. The initial configuration was constructed by adding another model molecular surface parallel to the initial surface in the converged configurations of water clusters interacting with a single surface. In the optimization process, the water molecule and the *z* coordinates of benzene which reflect the distance between the two surfaces were allowed to move freely (method A). Yet, the *x* and *y* coordinates of benzene are fixed. The surface represented by two benzene rings was chosen to model the confinement surfaces. The optimized geometries obtained using MP2/6-31G(d) calculations are shown in Figure 6.

The configuration of a water dimer, $(H_2O)_2$, confined within the model graphite surfaces is different from the case of water clusters interacting with one surface. Figure 6a shows that only one O−H bond points to the lower surface ($O_{41}H_{30}C_{18}$ is 171.787°) and one O−H points to the upper surface ($O_{41}H_{29}C_8$ is 171.640°) while the other two O−H bonds are parallel to the surfaces as well as the oxygen atoms. The O_{42}, H_{31}, and H_{32} are approximately at the same distance of 2.96 Å to the surfaces.

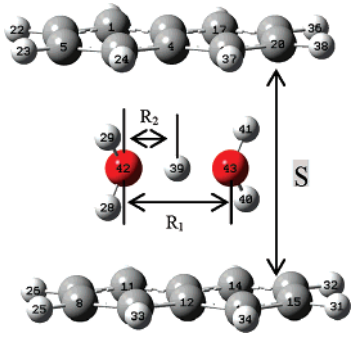

Figure 8. Optimal structure of $H_3O^+-(H_2O)$ confined within the model molecular surfaces.

However, there are two O−H bonds pointing to the surface in the case of one surface (Figure 3b). There is little symmetry of the water clusters related to the surfaces. The water molecule, $O_{42}H_{31}H_{32}$, forms one hydrogen bond with $O_{42}H_{31}\cdots O_{41}$, but H_{32} does not interact with the surroundings, while the other water molecule, $O_{41}H_{29}H_{30}$, forms the $O_{42}H_{31}\cdots O_{41}$ hydrogen bond, and both H_{29} and H_{30} interact with the surfaces. This may be a consequence that water clusters first tend to form the maximum hydrogen bonds and then the rest of the atoms attempt to interact with the surfaces. The distance between the oxygen atoms (Table 1) is 0.031 Å shorter and the hydrogen bond is 0.04 shorter than in the case of one surface. Therefore, the water−water interaction is slightly stronger in the confined environment. The average distances of O···surface and H···surface are approximately 0.06 and 0.31 Å shorter than the case of only one surface. Thus, the interaction between water molecules and the graphite surface is also stronger due to the confinement. The distance from the oxygen atoms to the upper and the lower surfaces is approximately equal at 3 Å, whereas the distance between the surfaces is ∼5.99 Å. Thus, the O_{41}, O_{42}, H_{31}, and H_{32} atoms locate at the middle between the model surfaces. The structure in Figure 6a shows two O−H bonds belonging to O_{42} that are parallel to the surface. This satisfies one of the preferential orientations of water molecules found from MD simulations.[8]

A water trimer between two surfaces shows the same arrangements as does the case with one surface (Figure 6b and Figure 4b, respectively). One O−H bond of each water molecule points to the surface where the angle of the O−H bond with the surface is nearly 180° ($O_{45}H_{33}C_3$ is 166.00°, $O_{44}H_{32}C_8$ is 178.67°, and $O_{43}H_{29}C_{12}$ is 172.50°), and hydrogen bonds are maximized by forming a cyclic network of them. As shown in Table 2, the O···O distance and hydrogen bond lengths are slightly shorter than the case of one surface, showing a littler stronger interaction between water molecules under a confinement environment. Also, the results of approximately 0.028 and

TABLE 3: Energy Barriers for Proton Transfer of the System Shown in Figure 8 in kcal/mol

		confined within the model molecular surfaces					
R_1 (Å)	no confinement	$S = 4$ Å	$S = 6$ Å	$S = 8$ Å	$S = 10$ Å	$S = 14.5$ Å	$S = 20$ Å
2.55	0.659	1.780	0.792	0.594	0.526	0.502	0.498
2.6	1.491	2.950	1.678	1.387	1.287	1.249	1.252
2.7	3.950	6.480	4.209	3.743	3.591	3.533	3.535
2.8	7.223	10.762	7.544	6.915	6.710	6.634	6.635
2.9	11.111	15.768	11.516	10.732	10.460	10.375	11.111
3.1	20.211	27.229	20.866	19.699	19.316	19.222	19.188

0.15 Å shorter O···surface and H···surface distances, compared to the case of one surface, suggest a stronger interaction between water molecules and the model graphite surface under confinement. The average distance between the two surfaces is 6.66 Å, and the oxygen atoms are approximately located in the middle between the graphite surfaces (approximately 3.1 Å between oxygen atoms and the lower and upper surfaces). Like the case of the confined water dimer, the water trimer does not show symmetry related to the molecular surfaces as there are two OH bonds interacting with the lower surface and one OH bond interacting with the upper surface. However, it is clear that the system makes an attempt to form a symmetric structure while maximizing the number of hydrogen bonds.

Figure 6c shows that a water tetramer between two graphite surfaces locates in the same arrangements as is the case with one surface, and two O−H pointing down to the lower surface ($O_{25}H_1C_{34}$ is 167.05°, $O_{28}H_8C_{10}$ is 162.64°), two O−H pointing up to the upper surfaces ($O_{26}H_4C_{45}$ is 158.82°, $O_{27}H_6C_{48}$ is 162.17°), and a square cyclic network of hydrogen bonds is formed. These square cycles of hydrogen bonds were also found in the MD simulations as shown in Figure 7 (left) in ref 8 maximizing hydrogen bonds. However, the configuration of two O−H bonds pointing down and two O−H bonds pointing away from one of the surfaces was not found in the MD results. This might be because the models of graphite surfaces in the MD are larger and the simulated water represents a higher density state. Also there are temperature effects that introduce variations to the optimal structure. The complex shows a symmetric geometry. All O···O distances and hydrogen bond lengths are shorter than in the case of one surface (Table 1), indicating that water−water interaction in confinement is stronger, similarly to the case of one, two, and three water molecules. The distance between the two surfaces is 6.87 Å, and the oxygen atoms are approximately 3.4 Å from the lower and upper surfaces. The average 0.068 and 0.101 Å shorter O···surface and H···surface distances, compared to the case of one surface, indicates a stronger interaction between water molecules and the model surface under a confined environment. Two from eight O−H bonds of four water molecules point to the lower surface, while four are parallel to the surface, and two of them point to the upper surface, indicating that they tend to be parallel to the model surface and maximize the hydrogen bonds rather than pointing toward the surface. This agrees with the structure found in the MD simulations with bulk water (Figure 3 in ref 8) and in particular with the fact that some hydrogen atoms locate closer to the model surface than the corresponding oxygen atoms (Figure 4 in ref 8). The structures shown in Figure 6, parts b and c, present one of the preferential orientations of water molecules, with one O−H pointing to the surface and the other parallel. However, it should be noted that the MD simulation system deals with high-density water, whereas here we have gas-phase water clusters.

Thus, water tetramers confined within model surfaces are likely to form symmetric configurations and the oxygen atoms locate approximately in the middle between the surfaces. At least one O−H bond of each water molecule is parallel to the surface. A cyclic network of hydrogen bonds is formed. Water−water interaction between two surfaces is stronger than in the case of one surface, and the water−graphite interaction is stronger as well. The distance between the surfaces increases with the number of water molecules. The MP2 calculations present both of the preferential orientations of water molecules as reported in the MD simulation, which involves condensed water, results[8] that one O−H points to the surface and the is other parallel and that both O−H bonds are parallel to the surface. Moreover, Lin et al.[30] have shown that both orientations of water molecules are present in the system of one surface of $(benzene)_7$ interacting with $(H_2O)_6$.

In the case of one water molecule confined between the two surfaces, as the structure is optimized, it evolves in such a way that the water molecule tries to escape from the confined space. Furthermore, the initial configurations of water clusters confined between the model surfaces were optimized by allowing *z* coordinates of every atom to move but restricting the *x* and *y* coordinates of every atom (method B). This means that the optimized structures of water clusters interacting with a model surface are fixed but the distances between them and the two surfaces are optimized. When the distances between the two surfaces of the two different optimization constraints are compared, the values are slightly different as shown in Table 2. The distances increase with the number of water molecules for both cases, but case B gives higher distance values. Also, the oxygen atoms locate approximately at the middle between the surfaces similarly to the case of water molecules moving freely. However, the energy values of method B are higher; thus, the structures are less stable.

Additional geometry optimizations were performed without any constraints. Although these cases do not represent a "graphite-type" confinement, they are of interest because it could correspond to cases found in amorphous carbon structures. The optimal geometries are shown in Figure 7. The arrangements of water clusters are similar to the case of only one surface, and the surfaces tend to arrange forming a T-shaped structure, which is one of the preferred configurations of the benzene dimer.[23,32−34] Therefore, the surface tends to interact with the other surface as well as with water clusters.

3.3. Proton Transfer between Two Water Molecules Confined within Model Molecular Surfaces. The initial configuration of a hydronium ion and a water molecule confined within model molecular surfaces was optimized using MP2/6-31G(d) under the constraints that all the coordinates of the hydronium ion and the water molecule, and the *z* coordinates of the surfaces, were allowed to be varied, whereas the *x* and *y* coordinates of the surfaces were restricted. The optimal geometry is shown in Figure 8. At the beginning, H_{39} was the hydrogen atom from the hydronium ion and belonged to O_{43}. The optimum distances between the oxygen atoms (R_1) and between oxygen and central hydrogen (R_2) are 2.42 and

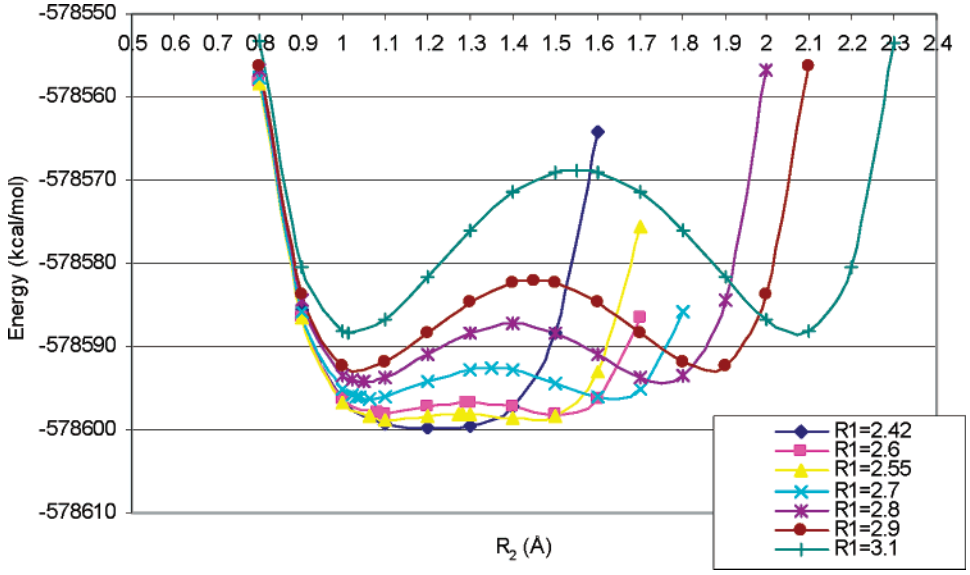

Figure 9. Energy of the system shown in Figure 8 at $S = 8$ Å.

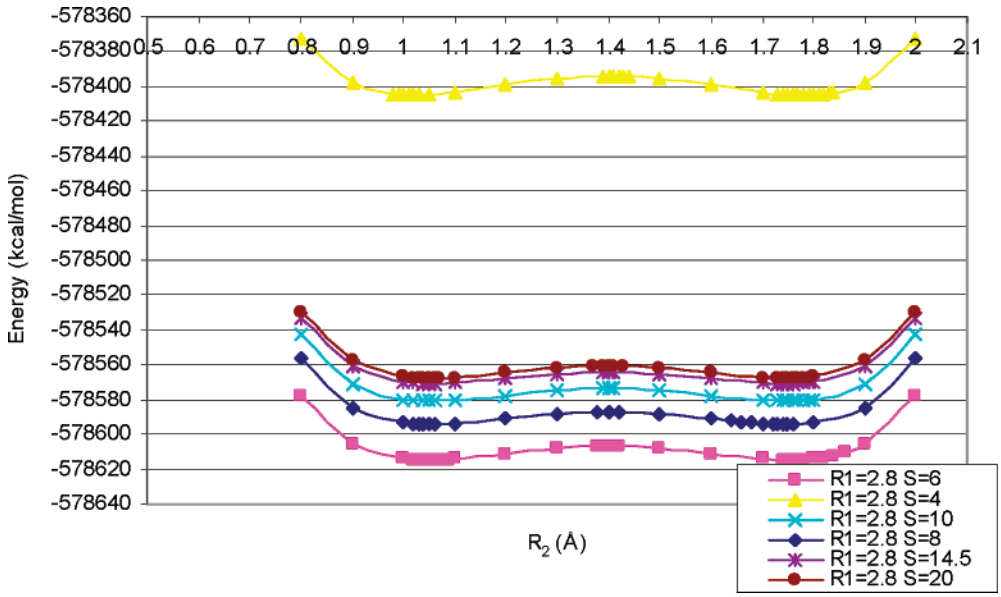

Figure 10. Energy of the system shown in Figure 8 at different S values and at the same R_1 of 2.8 Å.

TABLE 4: Interaction Energy of the H_3O^+ Confined within the Two Model Molecular Surfaces (kcal/mol)

S (Å)	interaction energy (kcal/mol)
4	137.182
6	1.438
8	21.604
10	33.582
14.5	43.177
20	45.520
25	46.233

1.21 Å, respectively, and the separation distance between the surfaces, S, is 5.89 Å. The oxygen atoms and H^+ locate at the middle between the surfaces and parallel to them.

The energy barriers for proton transfer from a hydronium ion in a confined environment as the proton propagates along the O−H···O hydrogen bond direction of the H_3O^+−(H_2O) complexes were determined. The distances R_1 were scanned at various S separations of 4, 6, 8, 10, 14.5, and 20 Å using the optimized geometry. The energy barrier (Table 3) is defined as the energy difference between the maximum located between

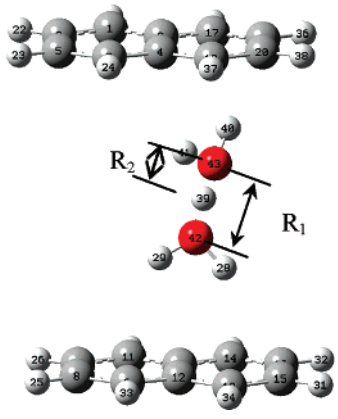

Figure 11. Another possible structure of H_3O^+−(H_2O) confined within the molecular surfaces, where the O···H···O direction is perpendicular to the surfaces.

minimum points of the curve having two minima (Figure 9). The left minimum energy points denote the equilibrium of a left H_3O^+ with a right H_2O. The symmetric minimum energy

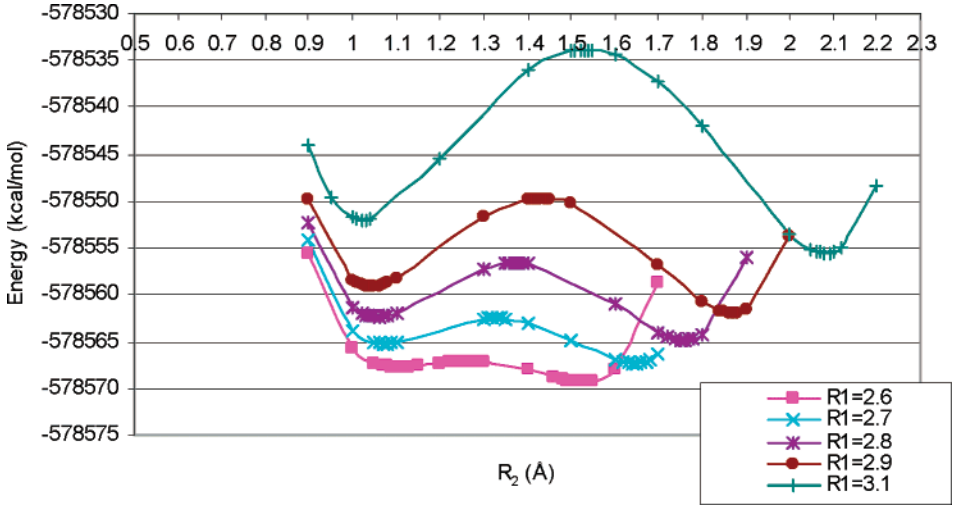

Figure 12. Energy of the system shown in Figure 11 at various R_1 and $S = 8$ Å.

TABLE 5: Energy Barriers for Proton Transfer of the System Shown in Figure 11 in kcal/mol[a]

R_1 (Å)	$S = 8$ (Å)	$S = 10$ (Å)	$S = 14.5$ (Å)	$S = 20$ (Å)
2.6	2.23 (*60.8*)	1.69 (*31.3*)	1.41 (*12.9*)	2.84 (*126.8*)
2.7	4.81 (*28.5*)	4.09 (*13.9*)	3.71 (*5.0*)	5.54 (*56.7*)
2.8	8.20 (*18.6*)	7.33 (*9.2*)	6.84 (*3.1*)	9.00 (*35.6*)
2.9	12.24 (*14.1*)	11.23 (*7.4*)	10.63 (*2.5*)	13.03 (*17.3*)
3.1	21.71 (*10.2*)	20.46 (*5.9*)	19.63 (*2.1*)	22.32 (*16.3*)

[a] The percentages of differences from the values shown in Table 3 are shown in italics between parentheses.

points at the right denote the equilibrium of a right H_3O^+ with a left H_2O. At a specific R_1, the maximum energy points give an estimate of the transition state of proton transfer. Figure 9 shows energy curves at different R_1 at $S = 8$ Å. The energy curves for other values of S show a similar trend: only when R_1 is at the optimal distance ($R_1 = 2.42$ Å), the curves show a single minimum for every S. Also, all other R_1 curves show symmetric double-well shapes similar to those found in the $H_3O^+-(H_2O)$ complexes in the unconfined environment.[28] Figure 10 shows that, at specific R_1 values, the system energy increases as H increases, but it shows a very small change at $S = 14.5$ and 20 Å. However, it rapidly increases when S is decreased to $S = 4$ Å.

Considering Table 3, as R_1 increases the energy barrier increases very sharply for every value of S. The energy barriers at $S = 4$ Å are the highest at every R_1 distance and increase sharply compared to the other S values and to the nonconfinement case. The energy barriers at $S = 6$ Å for every R_1 are only slightly higher than those of no confinement. At a specific R_1, when S is increasing between 6 and 14.5 Å, the energy barrier decreases. However, the energy barriers start increasing when S increases from 14.5 to 20 Å. The results suggest an interesting possibility that the confinement environment can either reduce or raise the barrier energy of proton transfer. At $S = 4$ Å, the $H_3O^+-(H_2O)$ complexes strongly interact with the surfaces. This might result in a higher energy requirement for a proton to overcome that strong interaction and to be transported from one molecule to another. The interaction energy of the simple example system of H_3O^+ confined between the two model surfaces has been calculated by subtracting the total energy of the system from the energy of H_3O^+, H_2O, and the surfaces. The results as shown in Table 4 show extremely strong repulsive interaction energy at $S = 4$ Å compared to the other H values. Additionally, it shows that at $S = 6$ Å, which is close to the optimum S, we find a very small repulsive value (1.44 kcal/mol). Also, as S is increased from 6 Å, the interaction energy is increasing, but it becomes almost constant when S is greater than 14.5 Å. Although the interaction energy is increasing between $S = 6-25$ Å, the energy barrier is reduced and starts to increase at $S = 20$ Å. Therefore, it suggests that at a specific range of surface separation between 6 and 14.5 Å the confinement effect somehow plays an important role on facilitating proton transport which does not only help to overcome the increasing repulsive interaction energy of the system but also creates even less energy barrier than that of the system of the least repulsive interaction energy ($S = 6$ Å). On the other hand, the confinement does not facilitate proton transfer when S is greater than 14.5 Å as the energy barrier begins to increase. It should be noted that the energy barrier has been calculated when the $H_3O^+-(H_2O)$ complexes are located in the middle between the surfaces. Thus, it implies that the complex does not feel the walls when S is greater than 14.5 Å. It was shown in results from MD simulations involving higher density water (Figure 3 in ref 8) that at $S = 14.5$ Å water molecules located in the middle of the pore (layers 2 and 3 of four) are not well ordered.

Furthermore, the energy barrier for proton transfer with another possible configuration of the $H_3O^+-(H_2O)$ complexes has been studied. The optimization of the $H_3O^+-(H_2O)$ complexes confined between the two model graphite sheets is performed at fixed $S = 8$ Å. The complexes tend to arrange as shown in Figure 11.

Unlike Figure 9, Figure 12 shows that the energy curves of every R_1 of the system, which are shown in Figure 11 at $S = 8$ Å, do not show the symmetric double-wells shape due to the asymmetric configuration of the system itself. Considering Table 5, the calculated barrier energy shows the same trend with the energy barrier found in the configuration shown in Figure 8. As R_1 is increasing, the energy barrier increases for every varied S. The energy barrier decreases when S is increasing between 8 and 14.5 Å, and it begins to increase at $S = 20$ Å. However, energy barriers shown in Table 5 are higher than those shown in Table 3 at the same S and R_1 (see the difference percents shown in parenthesis in Table 5).This result suggests that the arrangement shown in Figure 8 lowers the barriers for proton transfer compared to the arrangement shown in Figure 11.

Although the $H_3O^+-(H_2O)$ complexes at $S = 20$ Å are located closer to the surfaces than the configuration shown in Figure 8, the confinement does not encourage the proton transfer as the energy barrier begins to increase. At $S = 20$ Å, the

complexes are approximately 8 Å from the surfaces (Figure 11) and 9.5 Å (Figure 8). The complexes in Figure 8 with $S = 14.5$ Å are located approximately 6.5 Å from the surfaces, and the energy barriers decrease. Therefore, when the complexes are separated from the surfaces by more than 8 Å, the confinement ceases to benefit the proton transfer.

4. Conclusions

An analysis of the geometry of water clusters using ab initio calculations has been performed in an attempt to get new insights regarding the structure of confined water. The molecular model surfaces are represented by benzene and naphthalene molecules. The optimized geometries of $(H_2O)_n$ ($n = 1-4$) interacting with the molecular model surface are obtained by the ab initio MP2 and 6-31g(d) basis set. The results for benzene−water interaction structures obtained with MP2/6-31g(d) are in qualitative agreement with those results predicted by higher levels of theory and larger basis sets. The optimized geometries of the expanded surface model using a naphthalene molecule interacting to $(H_2O)_n$ ($n = 2-4$) exhibit slightly different arrangements from the case of using one benzene ring as a model surface. The stable configurations of water clusters interacting with a surface of two benzene rings show that water molecules locate nearly parallel to the surface and form a cyclic network of hydrogen bonds. Two O−H bonds from two water molecules point down to the surface, and at least one O−H bond points away from the surface for $n = 2-4$. Also, the water−water interaction is slightly stronger on the graphite surface than the isolated water molecules as the O···O separation and the hydrogen bond length are shorter.

Furthermore, the optimized geometries of $(H_2O)_n$ ($n = 2-4$) within naphthalene surfaces show fairly similar arrangements with the case of water clusters interacting with one surface. A cyclic network of hydrogen bonds is formed because the system attempts to maximize the number of hydrogen bonds. At least one O−H bond from one water molecule is parallel to the surfaces. The oxygen atoms locate approximately in the middle between the surfaces and are parallel to the surfaces. Symmetric structures of water clusters related to the surfaces are not found for the dimer and trimer water molecules, but it exists for the tetramer, where the system first tends to develop the maximum number of hydrogen bonds and then is likely to make a symmetric structure interacting with the surfaces. The MP2 calculations present the two most likely orientations of water molecules, which are found in previous MD simulation results,[7,8] that are (1) one O−H bond points to the surface and the other is parallel and (2) both O−H bonds are parallel to the surface. However, it should be noted that the models of graphite surfaces in the MD are much larger and the MD involves a condensed water phase. Furthermore, water−water interaction between two surfaces is stronger than in the case of one surface as the O···O distance and the hydrogen bond length are shorter. The water−graphite interaction is stronger because O···surface and H···surface distances are shorter.

Additionally, the energy barriers for proton transfer from a hydronium ion in a confined environment were calculated as the proton propagates along the O−H···O hydrogen bond direction of the $H_3O^+-(H_2O)$ complexes (with the O−H···O direction located parallel to the surfaces). The energy barriers were determined from the optimized configuration of a hydronium ion and a water molecule confined within the model surfaces using MP2/6-31G(d). As R_1 (the distance between the two oxygen atoms) increases, the energy barrier increases very sharply for every value of S, the separation between surfaces. At $S = 6$ Å, which is close to the optimal S (5.89 Å), the energy barriers are very close to those of the case of no confinement. The results show that as S is increased up to 14.5 Å, the energy barriers decrease, but they begin to increase at $S = 20$ Å. Therefore, it can be concluded that a specific range of S which the confinement helps to reduce the barrier energy of proton transfer is $S = 6-14.5$ Å. Also, when the system is highly confined at $S = 4$ Å, the energy barriers are extremely high due to very high interaction between the $H_3O^+-(H_2O)$ complexes and the surfaces. Moreover, the energy barriers for proton transfer were determined from another possible configuration of the $H_3O^+-(H_2O)$ complexes where the O−H···O direction is approximately perpendicular to the surfaces. The energy barriers show the same trend as with the other configuration but with higher values. In addition, the confinement in this configuration does not assist to lower the barrier energy of the proton transfer when the $H_3O^+-(H_2O)$ complexes are separated by more than 8 Å from each of the surfaces, which is manifested by an increase in the energy barriers at $S = 20$ Å.

Acknowledgment. Financial support from the U.S. Army Research Office and the U.S. Defense Threat Reduction Agency (DTRA) is gratefully acknowledged. P.H. thanks the National Nanotechnology Center of Thailand for providing a scholarship.

References and Notes

(1) Pertsin, A.; Grunze, M. *J. Phys. Chem. B* **2004**, *108*, 1357−1364.
(2) Koga, K.; Gao, G. T.; Tanaka, H.; Zeng, X. C. *Nature* **2001**, *412*, 802−805.
(3) Brennan, J. K.; Bandosz, T. J.; Thomson, K. T.; Gubbins, K. E. *Colloids Surf., A* **2001**, *187−188*, 539−568.
(4) Alberto, S.; Ariel, A. C.; Peter, T. C.; Keith, E. G. *J. Chem. Phys.* **2006**, *124*, 074710.
(5) Striolo, A.; Chialvo, A. A.; Gubbins, K. E.; Cummings, P. T. *J. Chem. Phys.* **2005**, *122*, 234712.
(6) Liu, J. C.; Monson, P. A. *Langmuir* **2005**, *21*, 10219−10225.
(7) Marti, J.; Nagy, G.; Gordillo, M. C.; Guardia, E. *J. Chem. Phys.* **2006**, *124*, 094703−094707.
(8) Hirunsit, P.; Balbuena, P. B. *J. Phys. Chem. C* **2007**, *111*, 1709−1715.
(9) Iiyama, T.; Nishikawa, K.; Suzuki, T.; Kaneko, K. *Chem. Phys. Lett.* **1997**, *274*, 152−158.
(10) Iiyama, T.; Nishikawa, K.; Otowa, T.; Kaneko, K. *J. Phys. Chem.* **1995**, *99*, 10075−10076.
(11) Striolo, A.; Naicker, P. K.; Chialvo, A. A.; Cummings, P. T.; Gubbins, K. E. *Adsorption* **2005**, *11*, 397−401.
(12) Werder, T.; Walther, J. H.; Jaffe, R. L.; Halicioglu, T.; Koumoutsakos, P. *J. Phys. Chem. B* **2003**, *107*, 1345−1352.
(13) Feller, D.; Jordan, K. D. *J. Phys. Chem. A* **2000**, *104*, 9971−9975.
(14) Fredericks, S. Y.; Jordan, K. D.; Zwier, T. S. *J. Phys. Chem.* **1996**, *100*, 7810−7821.
(15) Feller, D. *J. Phys. Chem. A* **1999**, *103*, 7558−7561.
(16) Purvis, G. D., III; Bartlett, R. J. *J. Chem. Phys.* **1982**, *76*, 1910−1918.
(17) Raghavachari, K.; Trucks, G. W.; Pople, J. A.; Head-Gordon, M. *Chem. Phys. Lett.* **1989**, *157*, 479−483.
(18) Watts, J. D.; Gauss, J.; Bartlett, R. J. *J. Chem. Phys.* **1993**, *98*, 8718.
(19) Christoph, D.; Mor, M. N.; Gerhard, H. *Phys. Rev. Lett.* **2003**, *90*, 105902.
(20) David, J. M.; Mathew, D. H. *Phys. Rev. Lett.* **2003**, *90*, 195503.
(21) Kreuer, K. D. *Chem. Mater.* **1996**, *8*, 610−641.
(22) Ruuska, H.; Pakkanen, T. A. *J. Phys. Chem. B* **2001**, *105*, 9541−9547.
(23) Hobza, P.; Selzle, H. L.; Schlag, E. W. *J. Phys. Chem.* **1996**, *100*, 18790−18794.
(24) Frisch, M. J.; Trucks, G. W.; Schlegel, H. B.; Scuseria, G. E.; Robb, M. A.; Cheeseman, J. R.; Montgomery, J. A., Jr.; Vreven, T.; Kudin, K. N.; Burant, J. C.; Millam, J. M.; Iyengar, S. S.; Tomasi, J.; Barone, V.; Mennucci, B.; Cossi, M.; Scalmani, G.; Rega, N.; Petersson, G. A.; Nakatsuji, H.; Hada, M.; Ehara, M.; Toyota, K.; Fukuda, R.; Hasegawa, J.; Ishida, M.; Nakajima, T.; Honda, Y.; Kitao, O.; Nakai, H.; Klene, M.; Li, X.; Knox, J. E.; Hratchian, H. P.; Cross, J. B.; Bakken, V.; Adamo, C.; Jaramillo, J.; Gomperts, R.; Stratmann, R. E.; Yazyev, O.; Austin, A. J.; Cammi, R.; Pomelli, C.; Ochterski, J. W.; Ayala, P. Y.; Morokuma, K.;

Voth, G. A.; Salvador, P.; Dannenberg, J. J.; Zakrzewski, V. G.; Dapprich, S.; Daniels, A. D.; Strain, M. C.; Farkas, O.; Malick, D. K.; Rabuck, A. D.; Raghavachari, K.; Foresman, J. B.; Ortiz, J. V.; Cui, Q.; Baboul, A. G.; Clifford, S.; Cioslowski, J.; Stefanov, B. B.; Liu, G.; Liashenko, A.; Piskorz, P.; Komaromi, I.; Martin, R. L.; Fox, D. J.; Keith, T.; Al-Laham, M. A.; Peng, C. Y.; Nanayakkara, A.; Challacombe, M.; Gill, P. M. W.; Johnson, B.; Chen, W.; Wong, M. W.; Gonzalez, C.; Pople, J. A. *Gaussian 03*, revision C.02; Gaussian, Inc.: Wallingford, CT, 2004.

(25) Suzuki, S.; Green, P. G.; Bumgarner, R. E.; Dasgupta, S.; Goddard, W. A.; Blake, G. A. *Science* **1992**, *257*, 942−944.

(26) Gutowsky, H. S.; Emilsson, T.; Arunan, E. *J. Chem. Phys.* **1993**, *99*, 4883−4893.

(27) Agmon, N. *Chem. Phys. Lett.* **1995**, *244*, 456−462.

(28) Li, T.; Wlaschin, A.; Balbuena, P. B. *Ind. Eng. Chem. Res.* **2001**, *40*, 4789−4800.

(29) Crofts, A. Lecture 12: Proton conduction, proton channels, proton wells. 1996, http://www.life.uiuc.edu/crofts/bioph354/lect12.html (accessed August, 2007).

(30) Lin, C. S.; Zhang, R. Q.; Lee, S. T.; Elstner, M.; Frauenheim, T.; Wan, L. J. *J. Phys. Chem. B* **2005**, *109*, 14183−14188.

(31) Xu, S.; Irle, S.; Musaev, D. G.; Lin, M. C. *J. Phys. Chem. A* **2005**, *109*, 9563−9572.

(32) Tsuzuki, S.; Honda, K.; Uchimaru, T.; Mikami, M.; Tanabe, K. *J. Am. Chem. Soc.* **2002**, *124*, 104−112.

(33) Smith, G. D.; Jaffe, R. L. *J. Phys. Chem.* **1996**, *100*, 9624−9630.

(34) Sinnokrot, M. O.; Valeev, E. F.; Sherrill, C. D. *J. Am. Chem. Soc.* **2002**, *124*, 10887−10893.